

# Do Fluorocarbon, Hydrocarbon, and Polycyclic Aromatic Groups Intermingle? Solution Properties of Pyrene-Labeled Bis(fluorocarbon/hydrocarbon)-Modified Poly(*N*-isopropylacrylamide)

Piotr Kujawa,<sup>†,§</sup> C. C. Ester Goh,<sup>‡</sup> Damien Calvet,<sup>†</sup> and Françoise M. Winnik<sup>\*,†,‡</sup>

Faculté de Pharmacie et Département de Chimie, Université de Montréal, C. P. 6128, succursale Centre-Ville, Montréal QC, Canada H3C 3J7; and Department of Chemistry, McMaster University, 1280 Main St W Hamilton ON, Canada L8S 4M1

Received March 2, 2001; Revised Manuscript Received June 14, 2001

**ABSTRACT:** Fluorescence spectroscopy, microcalorimetry, and isothermal titration calorimetry (ITC) have been used to study the solution properties in water of fluorocarbon, hydrocarbon, and bis(fluorocarbon/hydrocarbon) pyrene-labeled poly(*N*-isopropylacrylamides). The polymers were prepared by free-radical copolymerization in homogeneous solution of *N*-isopropylacrylamide, *N*-[4-(1-pyrenyl)butyl]-*N*-*n*-octadecylacrylamide, and/or *N*-(<sup>1</sup>H,<sup>1</sup>H-perfluoro-*n*-octylacrylamide). They were characterized by <sup>1</sup>H NMR and <sup>19</sup>F NMR spectroscopy, FTIR spectroscopy, and viscometry. Dynamic light scattering, ITC, and fluorescence spectroscopy provide strong evidence that the polymers associate in water below the solution cloud point (~30 °C). The polymers aggregate in multichain micellar structures consisting of a loose corona of hydrated poly(*N*-isopropylacrylamide) chains and a hydrophobic core composed of hydrocarbon, aromatic, and fluorocarbon groups. The fact that ground-state pyrene excimers are detected in aqueous solutions of bis(fluorocarbon/hydrocarbon)-modified polymers, *but not* in aqueous solutions of hydrocarbon-modified polymers, is taken as evidence for the segregation of fluorocarbon and hydrocarbon groups into distinct microdomains coexisting within the hydrophobic core of polymeric micelles.

## Introduction

Hydrophobically modified poly-(*N*-isopropylacrylamides) (HM-PNIPAM) obtained by random copolymerization of *N*-isopropylacrylamide (NIPAM) and *n*-alkylacrylamides were prepared in the early 1990s.<sup>1,2</sup> They dissolve readily in organic solvents where they adopt an extended conformation without any interpolymeric association, at least in the dilute regime. In contrast, in water HM-PNIPAM form polymeric micelles consisting of a viscous hydrophobic core formed by association of the *n*-alkyl groups and a loose corona of hydrated PNIPAM chains. Micellization takes place in very dilute solution. Depending on the chemical composition of the copolymer, the polymeric aggregates range in size from 20 to 50 nm and, in all cases, the association takes place between several polymer chains. When aqueous HM-PNIPAM solutions are heated above ~31 °C, phase separation occurs, a response to temperature characteristic of aqueous solutions of the homopolymer, PNIPAM.<sup>3</sup> The polymeric micelles are severely disrupted by the heating process: the hydrophobic core is destroyed and the alkyl chains are accommodated as isolated entities within the separated polymer-rich phase. This description of HM-PNIPAM aqueous solutions emanates from studies by dynamic light scattering and by fluorescence spectroscopy of pyrene- or naphthalene-labeled HM-PNIPAM samples, in which the chromophores are attached to the same monomer unit as the *n*-alkyl chain,<sup>1,4,5</sup> as well as from studies with extrinsic fluorescent probes, such as perylene<sup>1</sup> and

dipyme.<sup>6</sup> Other examples of hydrocarbon-modified PNIPAMs have been described recently. They include (i) polymers and oligomers of NIPAM carrying hydrophobic groups at one chain end,<sup>7–9</sup> and (ii) copolymers of NIPAM, *n*-alkylacrylamide and charged comonomers.<sup>10–13</sup>

The group of Jiang reported recently the synthesis of a series of fluorocarbon-modified poly(*N*-isopropylacrylamides) (PNIPAM-F) carrying from 0.06 to 1.50 mol % of C<sub>8</sub>F<sub>17</sub> chains.<sup>14,15</sup> Only polymers bearing less than 1 mol % of fluorocarbons are soluble in cold water. In all cases and even under conditions of very high dilution (~2 × 10<sup>-2</sup> g L<sup>-1</sup>), the fluorocarbon-modified polymers interact by an open association mechanism, involving an equilibrium between individual polymer chains and multichain aggregates. This observation is in agreement with the known enhanced hydrophobicity of fluorinated surfactants, compared to their hydrocarbon counterparts.<sup>16</sup> It confirms conclusions reached by Zhang et al.<sup>17</sup> that fluorocarbon-modified copolymers exhibit a more pronounced tendency toward aggregation than their hydrocarbon counterparts.

Water-soluble polymers carrying *both* fluorocarbon and hydrocarbon groups are expected to exhibit unique properties in aqueous solutions, as a result of the inherent lipophobic and hydrophobic nature of fluorocarbons, which leads to incompatibility of fluorinated and hydrogenated chains. Conceptually, such copolymers may form multicompartiment polymeric micelles (MCPM), a phrase coined by Ringsdorf<sup>18</sup> and de Gennes,<sup>19</sup> who compared their assembly to that of multidomain proteins. HM-polyacrylamides carrying both fluorocarbon (F) and hydrocarbon (H) groups were prepared by Strähler et al.<sup>20</sup> via terpolymerization of acrylamide with hydrocarbon and fluorocarbon monomeric surfactants incorporated in demixed fluorocarbon and hydrocarbon micelles. The presence of segregated H- and

\* To whom correspondence should be addressed (Université de Montréal address). E-mail: francoise.winnik@umontreal.ca. Telephone: (514) 343 6123. Fax: (514) 343 2362.

<sup>†</sup> Université de Montréal.

<sup>‡</sup> McMaster University.

<sup>§</sup> Permanent address: Institute of Applied Radiation Chemistry, Technical University of Lodz, Lodz, Poland.

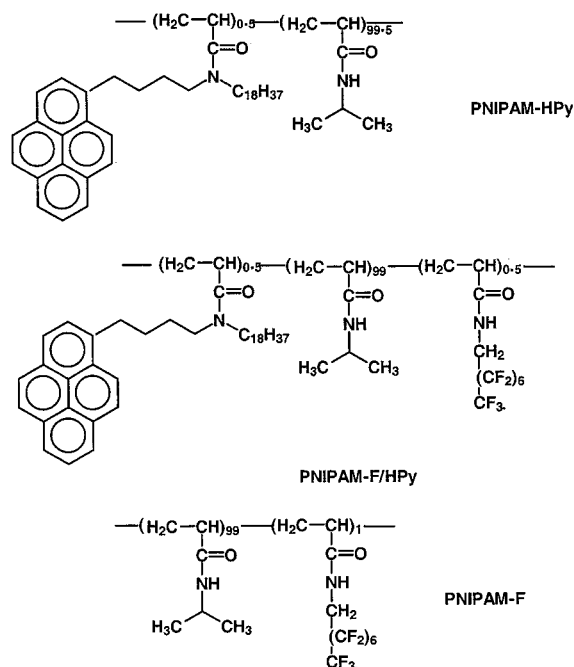


**Figure 1.** Chemical structure of the polymers used in this study.

F-microdomains in aqueous solutions of the H/F-terpolymers was inferred from viscosity and fluorescence probe experiments.

We report here another example of H/F hydrophobically modified terpolymers using the poly(*N*-isopropylacrylamide) backbone as the hydrophilic portion and  $^1\text{H}$ , $^1\text{H}$ -perfluorooctyl groups and *N*-(*n*-octadecyl)-*N*-[4-(1-pyrenyl)butyl] groups as mutually incompatible hydrophobic substituents. This terpolymer, PNIPAM-F/HPy (Figure 1), was obtained by free radical polymerization in homogeneous solution, taking advantage of the solubility in dioxane of NIPAM and the corresponding fluorocarbon and hydrocarbon acrylamides. Copolymers of NIPAM and either only perfluorinated substituents, PNIPAM-F, or only hydrocarbon substituents, PNIPAM-HPy, (Figure 1) were prepared under identical conditions. The copolymers were characterized by  $^1\text{H}$  NMR and  $^{19}\text{F}$  NMR. Their solution properties in water were studied by steady-state and time-resolved fluorescence spectroscopy, dynamic light scattering, turbidimetry, and microcalorimetry. Isothermal titration microcalorimetry was used to determine the polymer concentration at the onset of aggregation and the enthalpy of aggregation. On the basis of results gathered from the various experimental tools, we propose a model for the assembly in water of PNIPAM-F/HPy in which the chains form multipolymeric micelles composed of unique hydrophobic cores where hydrocarbon, fluorocarbon, and polycyclic aromatic groups coexist, albeit in segregated microdomains.

## Experimental Section

**Materials.** Water was deionized with a Millipore Milli-Q water purification system. Dioxane was distilled from sodium under nitrogen. Dichloromethane was dried over  $\text{MgSO}_4$  and distilled before use.  $^1\text{H}$ , $^1\text{H}$ -Perfluoro-*n*-octylamine was obtained from Lancaster Chemicals. Triethylamine (99%) was obtained from Anachemia. Acryloyl chloride and *N*-isopropylacrylamide were purchased from Aldrich Chemical Corp. 2,2'-Azobis(isobutyronitrile) (AIBN) was obtained from Spectrum Quality Products. Thin-layer chromatography (TLC) was performed with silica plates (Merck) eluted with  $\text{CH}_2\text{Cl}_2/\text{MeOH}$  (9/1 v/v).

**Monomer Synthesis.** *N*-[4-(1-Pyrenyl)butyl]-*N*-*n*-octadecylacrylamide was prepared as described previously.<sup>1</sup>

***N*-( $^1\text{H}$ , $^1\text{H}$ -Perfluoro-*n*-octylacrylamide).** Acryloyl chloride (0.5 mL, 0.454 g, 5.02 mmol) in dry dichloromethane (10 mL) was added over 30 min to a solution of  $^1\text{H}$ , $^1\text{H}$ -perfluoro-*n*-octylamine (2.056 g, 5.152 mmol) and triethylamine (0.75 mL, 0.545 g, 5.38 mmol) in dry dichloromethane (50 mL) kept in an ice bath. The reaction mixture was kept at room-temperature overnight. The precipitated triethylamine hydrochloride was separated by filtration. The filtrate was washed twice with water, and twice with saturated NaCl aqueous solution. It was dried over  $\text{MgSO}_4$ , filtered, and stripped of solvent in a rotary evaporator to yield *N*-( $^1\text{H}$ , $^1\text{H}$ -perfluoro-*n*-octylacrylamide) as a white solid (0.6 g, 26.5%):  $^1\text{H}$  NMR ( $\text{CDCl}_3$ ,  $\delta$ ) 4.11 (2H, dt,  $J_{\text{HF}}$  15.7 Hz,  $J_{\text{H-NH}}$  6.4 Hz,  $\text{NH-CH}_2\text{-CF}_2$ ), 5.78 (1H, dd,  $J$  1.4, 10.1 Hz,  $\text{H}_2\text{C=CH-}$ ), 5.89 (1H, br,  $\text{CO-NH}$ ), 6.16 (1H, dd,  $J_{\text{H-H}}$  16.9, 10.1 Hz,  $\text{CH}_2=\text{CH}$ ), 6.39 (1H, dd,  $J_{\text{HH}}$  1.42, 16.9 Hz,  $\text{H}_2\text{C=CH}$ ) ppm;  $^{19}\text{F}$  NMR ( $\text{CDCl}_3$ ,  $\delta$ ) -81.2 (3F, t,  $J_{\text{FF}}$  = 9.1 Hz,  $\text{CF}_3\text{-C}_6\text{F}_{12}$ ), -118.2 (2F, br,  $\text{-CH}_2\text{-CF}_2\text{-C}_5\text{F}_{11}$ ), -122.0 (2F, br,  $\text{CH}_2\text{-CF}_2\text{-CF}_2\text{-}$ ), -122.2 to -123.5 (6F, m), -126.3 (2F, m,  $\text{-CF}_2\text{-CF}_3$ ) ppm; FTIR (KBr) 3294 ( $\text{-CO-NH}$  stretching), 3080 ( $\text{H-C=}$ ), 1672 ( $\text{NH-C=O}$ ), 1637 ( $\text{C=C}$ ), 1556 ( $\text{CO-NH}$  bending)  $\text{cm}^{-1}$ .

**Polymerizations.** ***N*-Isopropylacrylamide-*N*-( $^1\text{H}$ , $^1\text{H}$ -perfluoro-*n*-octylacrylamide) Copolymer (PNIPAM-F).** A solution of NIPAM (2.277 g, 20 mmol) and *N*-( $^1\text{H}$ , $^1\text{H}$ -perfluoro-*n*-octylacrylamide) (0.097 g, 0.2 mmol) in dry dioxane (20 mL) was degassed with nitrogen for 15 min. It was heated to 65 °C. AIBN (0.01 g, 0.06 mmol) was added at once to initiate the polymerization, which was carried out for 48 h at 65 °C. The polymer was recovered by precipitation into diethyl ether. It was purified by two precipitations from THF into diethyl ether and dried in vacuo for 24 h (2.3 g, 97%):  $^1\text{H}$  NMR ( $\text{CDCl}_3$ ,  $\delta$ ) 1.14–1.20 (br s, isopropyl methyl protons), 1.24–2.44 (m,  $\text{-CH}_2\text{-CH-}$ ), 4.00 (br s,  $(\text{CH}_3)_2\text{CH-NH}$ ,  $\text{-CF}_2\text{-CH}_2\text{-NH}$ ), 6.17 (br s,  $\text{NH-CO}$ ) ppm;  $^{13}\text{C}$  NMR ( $\text{CDCl}_3$ ,  $\delta$ ) 22.78 (isopropylmethyl carbons), 174.2 ( $\text{-CO-NH-}$ ) ppm;  $^{19}\text{F}$  NMR ( $\text{CDCl}_3$ ,  $\delta$ ) -82.3 (br t,  $\text{CF}_3\text{-C}_6\text{F}_{12}$ ), -119.4 (br,  $\text{-CH}_2\text{-CF}_2\text{-C}_5\text{F}_{11}$ ), -123.3 (br,  $\text{CH}_2\text{-CF}_2\text{-CF}_2\text{-}$ ), -123.6 to -123.5 (m,  $\text{-CH}_2\text{-CF}_2\text{-(CF}_2)_3\text{-CF}_2\text{-CF}_3$ ), -127.7 (m,  $\text{-CF}_2\text{-CF}_3$ ) ppm.

***N*-Isopropylacrylamide-*N*-( $^1\text{H}$ , $^1\text{H}$ -perfluorooctylacrylamide)-*N*-[4-(1-pyrenyl)butyl]-*N*-*n*-octadecylacrylamide) Copolymer (PNIPAM-F/HPy).** The copolymer was obtained under the same conditions as PNIPAM-F, starting with NIPAM (2.251 g, 20 mmol), *N*-( $^1\text{H}$ , $^1\text{H}$ -perfluoro-*n*-octylacrylamide) (0.0528 g, 0.12 mmol), *N*-[4-(1-pyrenyl)butyl]-*N*-*n*-octadecylacrylamide (0.0635 g, 0.11 mmol), and AIBN (0.01 g, 0.06 mmol). The polymer was purified by repeated precipitations from THF into diethyl ether (2.35 g, 95%):  $^1\text{H}$  NMR ( $\text{CDCl}_3$ ,  $\delta$ ) 0.875 (t,  $\text{CH}_3\text{-C}_{17}\text{H}_{34}$ ), 1.14–1.20 (br s, isopropylmethyl protons), 1.25–2.44 (br m,  $\text{-CH}_2\text{-CH-}$  and  $\text{CH}_2$  of the octadecyl chain), 4.007 (br s,  $(\text{CH}_3)_2\text{CH-NH}$ ,  $\text{-CF}_2\text{-CH}_2\text{-NH}$ ), 6.184 (br s,  $\text{NH-CO}$ ), m centered at 8.10 (pyrenyl protons);  $^{19}\text{F}$  NMR ( $\text{CDCl}_3$ ,  $\delta$ ) -82.27 (br t,  $\text{CF}_3\text{-(CF}_2)_6\text{-}$ ), -119.45 (br,  $\text{-CH}_2\text{-CF}_2\text{-C}_5\text{F}_{11}$ ), -123.3 (br,  $\text{CH}_2\text{-CF}_2\text{-CF}_2\text{-}$ ), -123.6–125.7 (m,  $\text{-CH}_2\text{-CF}_2\text{-(CF}_2)_3\text{-CF}_2\text{-}$ ), -127.66 (m,  $\text{-CF}_2\text{-CF}_3$ ) ppm.

**Instrumentation.** Proton NMR spectra were recorded on Bruker 300 and 500 MHz spectrometers. The chemical shifts are referenced to trimethylsilane (TMS).  $^{13}\text{C}$  NMR spectra were recorded on a Bruker 200 MHz spectrometer. They were referenced to TMS.  $^{19}\text{F}$  NMR spectra were recorded on a Bruker 400 MHz spectrometer. The chemical shifts of  $^{19}\text{F}$  signals were referenced to external  $\text{CFCl}_3$ . The acquisition parameters were as follows: spectral width, 83 333 Hz; relaxation delay, 1.0 s; acquisition time, 0.811 s; pulse time, 10  $\mu\text{s}$ . Infrared spectra were recorded on a BioRad FTS-40 spectrometer. UV spectra were measured with a Hewlett-Packard 8452A photodiode array spectrometer. Viscometry measurements were carried out with an Ubbelohde viscometer kept at 27 °C. Dynamic light scattering was performed on a Brookhaven BI9000 AT instrument equipped with an argon laser ( $\lambda = 514 \text{ nm}$ ; scattering angle, 90°). The measurements were performed at 20 °C using polymer solutions (1.0 g  $\text{L}^{-1}$ ) equilibrated at room temperature for 24 h and filtered through

a 0.45  $\mu\text{m}$  membrane prior to measurements. Data were analyzed using the software provided by the manufacturer (CONTIN calculations).

**Cloud Point Determinations.** Cloud points were determined by spectrophotometric detection of the changes in turbidity ( $\lambda = 600 \text{ nm}$ ) of aqueous polymer solutions ( $1.0 \text{ g L}^{-1}$ ) heated at a constant rate ( $0.5 \text{ }^\circ\text{C min}^{-1}$ ) in a magnetically stirred UV cell. The value reported is the temperature corresponding to a decrease of 20% of the solution transmittance.

**Differential Scanning Calorimetry (DSC).** DSC measurements were performed on a VP-DSC microcalorimeter (MicroCal Inc) at an external pressure of ca. 180 kPa. The cell volume was 0.517 mL. The heating rate was  $1.5 \text{ }^\circ\text{C min}^{-1}$ , and the instrument response time was set at 5.6 s. Data were corrected for instrument response time and analyzed using the software supplied by the manufacturer. The polymer concentration was  $1.0 \text{ g L}^{-1}$ .

**Pressure Perturbation Calorimetry (PPC).** PPC measurements were performed on a VP-DSC microcalorimeter equipped with a pressure perturbation accessory (MicroCal Inc). The pressure applied during the compression cycle was 500 kPa. The reference cell and sample cell volumes were identical (0.517 mL). The polymer concentration was  $5.0 \text{ g L}^{-1}$ . Data were analyzed as described previously,<sup>21</sup> using the software supplied by the manufacturer.

Pressure perturbation calorimetry (PPC) measures the heat change resulting from a pressure change above a polymer solution. This heat change can be used to calculate  $\alpha_p$ , the coefficient of thermal expansion of the solute, eq 1, where  $T$  and  $V$  are the temperature and volume, respectively. From the temperature dependence of  $\alpha_p$ , one can determine the partial specific volume of a polymer in solution  $\bar{V}_p$ , which can be expressed as a function of  $V_M$ , the intrinsic polymer volume and  $\Delta V_h$ , the volume effect of hydration, that is the polymer-induced change in solvent volume (eq 2).

$$\alpha_p = \frac{1}{V} \left( \frac{\partial V}{\partial T} \right)_P \quad (1)$$

$$\bar{V}_p = V_M + \Delta V_h \quad (2)$$

**Isothermal Titration Calorimetry (ITC).** ITC measurements were performed using a VP-ITC titration microcalorimeter (MicroCal Inc.). The sample cell had a volume of 1.43 mL. A solution of a polymer ( $5.0 \text{ g L}^{-1}$ ) was titrated into water placed in the sample cell. The injection volume was  $5 \mu\text{L}$ . A total of 58 consecutive injections were performed. The delay time between two consecutive injections was 300 s. All measurements were carried out at  $25 \text{ }^\circ\text{C}$ . Data were analyzed using the Microcal ORIGIN software. The results are presented in terms of the enthalpy evolved per mole of injectant (NIPAM unit) as a function of the total injectant concentration. The principles and basic thermodynamic conventions of ITC are discussed in a recent publication.<sup>22</sup>

The enthalpograms were analyzed as follows:<sup>33</sup> A linear fit of the data sets in the lower and upper concentration domains was performed. The abscissas of the last (highest) value in the fitted raw data of the lower concentration range, ST, and of the first (lowest) value in the fitted data of the higher concentration domain, ET, were taken as the polymer concentrations corresponding to the start and end of micellization, respectively. The intercepts of the two straight lines were determined. The difference of the two intercepts yielded the enthalpy of demicellization (Figure 2).

**Fluorescence Measurements.** Steady-state fluorescence spectra were recorded on a SPEX Industries Fluorolog 212 spectrometer equipped with a GRAMS/32 data analysis system. Temperature control of the samples was achieved using a water-jacketed cell holder connected to a Neslab circulating bath. The temperature of the sample fluid was measured with a thermocouple immersed in a water-filled cuvette placed in one of the four cell holders in the sample compartment. All measurements were carried out at  $25 \text{ }^\circ\text{C}$  unless otherwise stated. The slit settings were 0.5 mm (excitation) and 2.0 mm

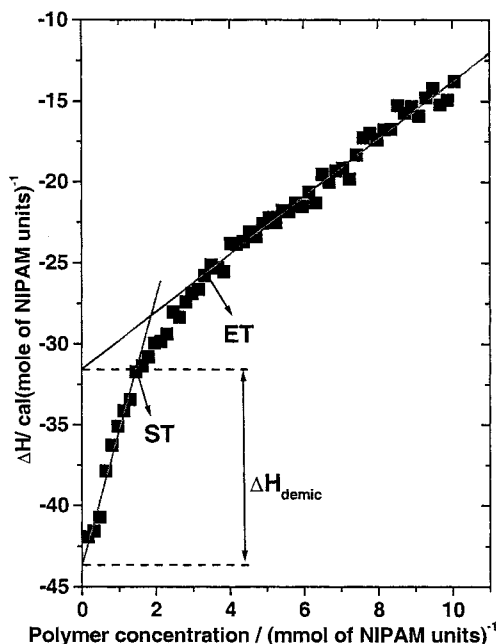


**Figure 2.** Determination of the enthalpy of demicellization ( $\Delta H_{\text{demic}}$ ) and the concentrations ST and ET from an experimental enthalpogram obtained for a titration of PNIPAM-F ( $5 \text{ g L}^{-1}$ ) in water at  $25 \text{ }^\circ\text{C}$ .

(emission). Emission spectra were recorded with an excitation wavelength of 346 nm. Excitation spectra were measured in the ratio mode. They were monitored at 378 nm (monomer emission) and 485 nm (excimer emission). Samples for analysis, prepared from stock solutions ( $5.0 \text{ g L}^{-1}$ ), had a polymer concentration of  $0.05 \text{ g L}^{-1}$ . Solutions were kept in the dark at  $5 \text{ }^\circ\text{C}$  for 12 h prior to measurements. Solutions in water were not degassed. Solutions in methanol were degassed by vigorous purging (1 min) with methanol-saturated argon. The pyrene excimer-to-monomer ratio ( $I_E/I_M$ ) was calculated by taking the ratio of the intensity (peak height) at 480 nm to the intensity of the half-sum of the intensities at 380 and 400 nm.

Fluorescence lifetimes were measured on a Fluorolog-Tau-3 multifrequency phase modulation fluorometer (Jobin-Yvon Horiba Inc). The excitation light from a 450 W xenon lamp was modulated with a Pockels cell. Phase and modulation values were determined relative to a glycogen aqueous solution. The excitation wavelength was set at 346 nm. Pyrene monomer and excimer emissions were monitored at 376 and 480 nm, respectively. The frequency of the analyzing light was chosen in the range of 0.1 to 100 MHz. All measurements were carried out at  $25 \text{ }^\circ\text{C}$ . Data were analyzed with the Datamax Spectroscopy software based on GRAMS/32 from Galactic Ind. Data were fit to a multiexponential decay law,  $F(t) = \sum a_i e^{-t/\tau_i}$ , where  $a_i$  and  $\tau_i$  are the preexponential factors and the lifetime of the  $i$ th component, respectively. The goodness of the fit was determined by the  $\chi^2$  value and examination of the residuals. The preexponential factors  $a_i$  are related to the observed fractional intensity contribution  $f_i$  by the relation  $f_i = a_i \tau_i / \sum a_j \tau_j$ . The average lifetime  $\langle \tau \rangle$  was calculated from  $\langle \tau \rangle = f_1 \tau_1 + f_2 \tau_2$ .

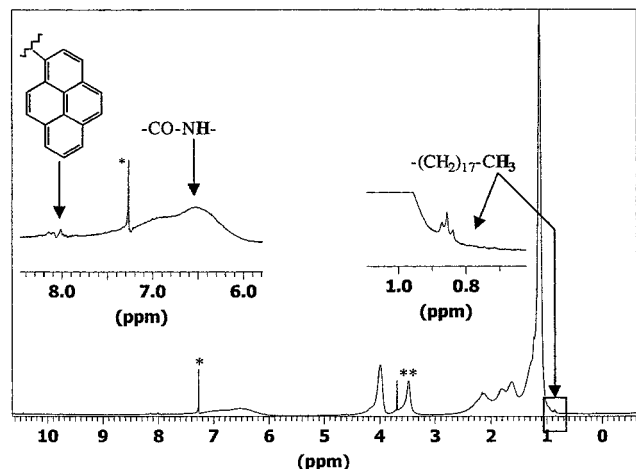
## Results and Discussion

**Preparation and Characterization of the Polymers.** All copolymers were obtained by free radical polymerization of NIPAM and the respective hydrocarbon or fluorocarbon-modified acrylamides. The reaction was done in dry dioxane, a solvent in which both monomers and polymers are soluble. These conditions were selected to favor statistical growth of the copolymers and to achieve control of the polymer composition



Table 1. Physical Properties of the Polymers Investigated

polymer	composition (mol %)				$[\eta]$ (mL g <sup>-1</sup> )	$M_v^a$	ref
	NIPAM	C <sub>18</sub> H <sub>37</sub>	CH <sub>2</sub> C <sub>7</sub> F <sub>15</sub>	Py			
PNIPAM	100				39.0	360 000	1
PNIPAM-F	99		1		24.0	180 000	this work
PNIPAM-HPy	99.5	0.5		0.5	41.3	390 000	1
PNIPAM-F/HPy	99	0.5	0.5	0.5	20.4	130 000	this work

<sup>a</sup> From viscosity in THF.

**Figure 3.** <sup>1</sup>H NMR spectrum of PNIPAM-F/HPy in CDCl<sub>3</sub>. The asterisks indicate signals due to CHCl<sub>3</sub> (7.3 ppm) and residual H<sub>2</sub>O (3.4 to 3.8 ppm).

by the initial monomer feed ratios. Molecular weights of the purified copolymers were estimated from the intrinsic viscosity of polymer solutions in THF, using the relationship  $[\eta] = 9.59 \times 10^{-3} M_{vis}^{0.65}$ , established for PNIPAM<sup>23</sup> and assumed to be valid also for the copolymers prepared here (Table 1). The chemical composition of the copolymers was ascertained by NMR spectroscopy. The <sup>1</sup>H NMR spectrum of PNIPAM-F/HPy in CDCl<sub>3</sub> (Figure 3) presents a well-resolved triplet at  $\delta$  0.87 ppm, attributed to the resonance of the terminal methyl protons of the octadecyl chain and a broad singlet at  $\delta$  4.0 ppm, attributed to the resonances of the NIPAM residue methine protons and the methylene protons of the perfluorochain. These two signals were used to determine the level of *N*-4-[1-(pyrenyl)butyl]-*N*-octadecyl group incorporation (0.5 mol % or  $\sim 4.2 \times 10^{-5}$  mol g<sup>-1</sup> polymer).<sup>24</sup> This value was confirmed by UV absorption data of a polymer solution in methanol, using *N*-4-[1-(pyrenyl)butyl]-*N*-octadecylacrylamide ( $\epsilon_{314} = 34\,900$  cm<sup>-1</sup> mol<sup>-1</sup> L)<sup>1</sup> as reference compound.

The <sup>1</sup>H NMR spectrum of PNIPAM-F/HPy could not be used to assess the level of perfluorochain incorporation, due to the unfortunate overlap of the NIPAM methine proton and perfluorooctyl methylene protons resonances ( $\delta \sim 4.0$  ppm). Evidence for the presence of perfluorooctyl groups was provided by the <sup>19</sup>F NMR spectrum of PNIPAM-F/HPy in CDCl<sub>3</sub> displayed in Figure 4, together with the <sup>19</sup>F NMR spectrum of *N*-<sup>1</sup>H,<sup>1</sup>H-perfluoro-*n*-octylamine. We note that the multiplet centered at  $\delta = -122.15$  ppm, attributed to the resonance of the C<sub>2</sub> fluorines in the spectrum of the amine, undergoes a downfield shift ( $\delta = -119.4$  ppm) and significant broadening in the spectrum of PNIPAM-F/HPy. In addition, the triplet ( $\delta = -82.27$  ppm,  $J_{FF} = 9.1$  Hz) attributed to the terminal CF<sub>3</sub> is broader and shifted to higher field, compared to the spectrum of the starting amine ( $\delta = -81.18$  ppm).<sup>25</sup> Both observations

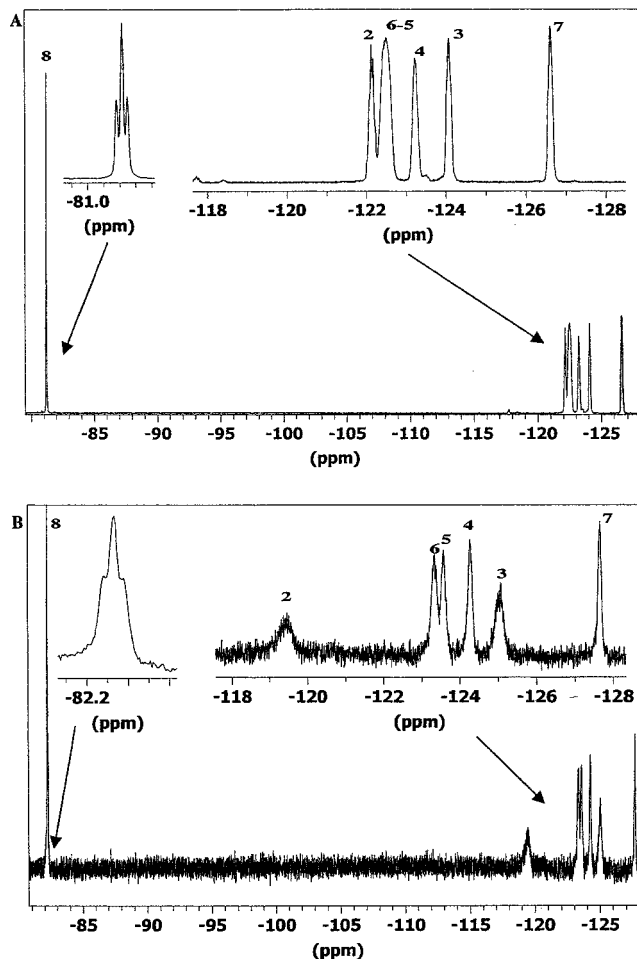


**Figure 4.** <sup>19</sup>F NMR spectra of *N*-<sup>1</sup>H,<sup>1</sup>H-perfluorooctylamine (A) and PNIPAM-F/HPy (B) in CDCl<sub>3</sub>. The digits labeling the signals correspond to the numbers assigned to each carbon along the chain, i.e.: C(8)F<sub>3</sub>-C(7)F<sub>2</sub>-C(6)F<sub>2</sub>-C(5)F<sub>2</sub>-C(4)F<sub>2</sub>-C(3)F<sub>2</sub>-C(2)F<sub>2</sub>-C(1)H<sub>2</sub>-NHR.

provide conclusive evidence for the linking of the fluorocarbon chain to the polymer backbone but do not give quantitative information on the level of fluorocarbon incorporation, which is assumed to be identical to the monomer feed ratio.

**Thermal Properties of Aqueous Polymer Solutions.** The copolymers reported here were soluble in water at room temperature or below.<sup>26</sup> Aqueous solutions became turbid when heated above their cloud point. The temperatures of phase separation, determined by changes in solution transmittance at 600 nm, a wavelength of light absorbed neither by the solvent nor by the polymers, range from 30.0 to 31.8 °C (Table 2). The values are identical, within experimental error, to the cloud point of aqueous PNIPAM solutions. The fact that they do not reflect the increased hydrophobicity of the modified copolymers suggests that the hydrophobic groups are not exposed to water but form

**Table 2. Cloud Points and Microcalorimetry Data on the Phase Transition of Aqueous Solutions of HM-PNIPAM Samples**

polymer	cloud point <sup>a</sup> (°C)	$T_m$ <sup>b</sup> (°C)	$\Delta T_{1/2}$ (°C)	$\Delta H$ (kcal mol <sup>-1</sup> NIPAM)	$\Delta C_p$ (cal mol <sup>-1</sup> °C)
PNIPAM	31.8 ± 0.3	33.7 ± 0.2	2.4 ± 0.2	1.4 ± 0.2	-15 ± 2
PNIPAM-HPy	31.7 ± 0.3	31.7 ± 0.2	2.0 ± 0.2	1.1 ± 0.2	-20 ± 2
PNIPAM-F	30.0 ± 0.3	30.0 ± 0.2	4.0 ± 0.2	1.0 ± 0.2	-25 ± 2
PNIPAM-F/HPy	30.0 ± 0.3	30.4 ± 0.2	4.8 ± 0.2	1.1 ± 0.2	-25 ± 2

<sup>a</sup> Values determined by turbidimetry; <sup>b</sup> temperature of the transition maxima determined by DSC.

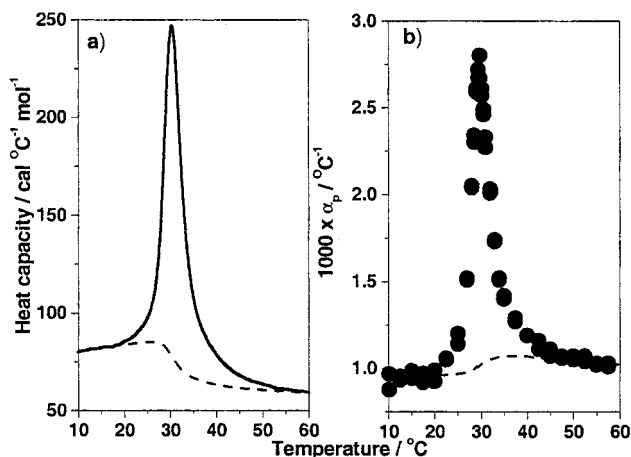


**Figure 5.** (a) Microcalorimetric endotherm for an aqueous solution of PNIPAM-F/HPy (1.0 g L<sup>-1</sup>) in H<sub>2</sub>O; heating rate, 1 °C min<sup>-1</sup>. (b) Temperature dependence of the coefficient of thermal expansion ( $\alpha_p$ ) of PNIPAM-F/HPy in H<sub>2</sub>O (polymer concentration: 5.0 g L<sup>-1</sup>). The dotted lines represent the progress baseline.

hydrophobic microdomains protected from the water by the PNIPAM chains. The latter undergo heat-induced dehydration and collapse by the same mechanism as PNIPAM homopolymer.

The temperature dependence of the partial heat capacity of aqueous HM-PNIPAM solutions was monitored by microcalorimetry in an attempt to detect subtle differences among the thermodynamic parameters of the phase transition for the three polymers investigated. Figure 5a shows the thermogram associated with the phase transition of aqueous PNIPAM-F/HPy. The plot yields three parameters: the temperature of maximum heat capacity ( $T_m$ ), the heat of transition ( $\Delta H$ ), and the difference of the heat capacity ( $\Delta C_p$ ) of the PNIPAM-F/HPy solution before and after the phase transition. These values, together with  $\Delta T_{1/2}$ , the width of the transition at half-height, are listed in Table 2 for PNIPAM and the three copolymers. We note that the transition is broader in the case of the fluorocarbon-modified copolymers but that the enthalpy of the transition per NIPAM unit ( $\sim 1.0$  kcal mol<sup>-1</sup>) is the same in all cases. It is consistent with the loss of approximately one hydrogen bond per repeat unit.<sup>27</sup> It can be seen in Figure 5a that the heat capacity of PNIPAM-F/HPy at high temperature is smaller than that of the polymer solution at low temperature, as is the case also for PNIPAM solutions (Table 2). The decrease in heat capacity indicates that the collapse of the polymer causes a decrease in the number of polymer/water contacts, in analogy with the refolding of proteins upon heat after cold denaturation.<sup>28</sup> Interestingly, the amplitude of the change in solution heat capacity before and after the transition,  $\Delta C_p$ , is larger for solutions of the modified polymers, compared to PNIPAM. This effect hints at differences in polymer/water interactions,

even though the temperature and heat of the transition seem unaffected by hydrophobic substitution.

Additional information on the solvation layer around the polymer was obtained by another calorimetric technique, known as pressure perturbation calorimetry (PPC), which measures the heat change resulting from a pressure change above a polymer solution.<sup>21</sup> This heat change can be used to calculate the coefficient of thermal expansion of a solute. If the measurements are carried out on solutions that undergo temperature-induced phase transitions, it is possible to evaluate the changes in the volume of the polymer solvation layer before and after the phase transition. A PPC scan recorded with a solution of PNIPAM-F/HPy in water (Figure 5b) presents the changes with temperature of the thermal expansion coefficient of the polymer ( $\alpha_p$ ). The plot can be divided into three temperature ranges. Below the transition temperature,  $15 < T < 30$  °C, and above that temperature,  $45 < T < 80$  °C,  $\alpha_p$  exhibits a slight sensitivity to changes in temperature. Around the phase transition temperature  $\alpha_p$  undergoes a sharp increase, reaches a maximum at  $T_m$ , and then rapidly decreases with further increase in temperature. The plots recorded for PNIPAM and the other HM-PNIPAM samples present similar features, except that the thermal expansion coefficient of PNIPAM is significantly larger after the transition temperature, while in the case of the hydrophobically modified polymers, values of  $\alpha_p$  remain constant before and after the transition. Values of  $\alpha_p$  recorded at 15, 25, and 50 °C for aqueous solutions of the three HM-PNIPAM samples, for PNIPAM, and for water are listed in Table 3.

Integration of the changes of  $\alpha_p$  with temperature yields  $\Delta V/V$ , the change in volume of the polymer solvation layer, corresponding to the collapse of the PNIPAM chain, where  $V$  is the total volume occupied by a solvated polymer chain. In these data treatments, we assume that the intrinsic volume occupied by a polymer chain remains constant in the temperature range studied.<sup>21</sup> The volume changes, expressed as percent of the total polymer volume,  $\Delta V/V$ , are listed in Table 3. We note that the amplitude of the volume change is largest in the cases of PNIPAM-F and PNIPAM-F/HPy. The enhanced changes in hydration volume in the case of fluorocarbon-modified polymers may indicate that there is a higher level of ordering of the water molecules bound to the polymer chains and hence a larger volume of directly interacting water. In all cases, however, the volume changes are quite large in comparison with those measured during the heat-induced protein denaturation, a phenomenon usually accompanied by  $\Delta V/V$  on the order of 0.1%.<sup>21</sup>

**Micellar Properties of the Copolymers.** While the <sup>1</sup>H NMR and <sup>19</sup>F NMR spectra of all the copolymers in CDCl<sub>3</sub>, a good solvent for PNIPAM, were well-resolved (see Figures 3 and 4), <sup>1</sup>H NMR spectra run with copolymers D<sub>2</sub>O solution exhibited significant broadening of certain signals, particularly the triplet at  $\delta$  0.82

**Table 3. Thermodynamic Characteristics of Aqueous Solutions of HM-PNIPAM Samples Determined by Pressure Perturbation Calorimetry**

polymer	$T_m$ (°C)	$\Delta V/V$ (%)	$\alpha_{p15}$ (K <sup>-1</sup> )	$\alpha_{p25}$ (K <sup>-1</sup> )	$\alpha_{p50}$ (K <sup>-1</sup> )	$\Delta\alpha_p$ (K <sup>-1</sup> ) <sup>a</sup>
PNIPAM	33.70 ± 0.5	1.010 ± 0.005	$0.76 \times 10^{-3}$	$0.88 \times 10^{-3}$	$1.28 \times 10^{-3}$	$0.52 \times 10^{-3}$
PNIPAM-HPy	29.50 ± 0.5	1.040 ± 0.005	$0.86 \times 10^{-3}$	$0.96 \times 10^{-3}$	$0.93 \times 10^{-3}$	$0.07 \times 10^{-3}$
PNIPAM-F	30.00 ± 0.5	1.200 ± 0.005	$0.98 \times 10^{-3}$	$1.04 \times 10^{-3}$	$1.00 \times 10^{-3}$	$0.02 \times 10^{-3}$
PNIPAM-F/HPy	29.00 ± 0.5	1.090 ± 0.005	$0.97 \times 10^{-3}$	$1.16 \times 10^{-3}$	$1.06 \times 10^{-3}$	$0.09 \times 10^{-3}$
H <sub>2</sub> O			$1.503 \times 10^{-4}$	$2.578 \times 10^{-4}$	$4.571 \times 10^{-4}$	$0.07 \times 10^{-3}$

$$^a \Delta\alpha_p = \alpha_{p50} - \alpha_{p15}.$$

**Table 4. Micellar Properties of the HM-PNIPAM Samples in Water**

polymer	PNIPAM-F	PNIPAM-F/HPy	PNIPAM-HPy
aggregate size (nm)	20 ± 2	22 ± 2	38 ± 2 <sup>d</sup>
ST <sup>a</sup> (mol NIPAM L <sup>-1</sup> )	$1.5 \times 10^{-3}$	$1.0 \times 10^{-3}$	<i>c</i>
ST (g L <sup>-1</sup> )	0.17	0.12	
ST (mol C <sub>7</sub> F <sub>15</sub> )	$1.3 \times 10^{-5}$	$0.7 \times 10^{-5}$	
ET <sup>b</sup> (mol NIPAM L <sup>-1</sup> )	$3.2 \times 10^{-3}$	$2.3 \times 10^{-3}$	<i>c</i>
ET (g L <sup>-1</sup> )	0.36	0.27	
ET (mol C <sub>7</sub> F <sub>15</sub> )	$3.0 \times 10^{-5}$	$1.1 \times 10^{-5}$	
$\Delta H_{demic}$ [cal (mol <sup>-1</sup> NIPAM)]	-10	-11	<i>c</i>
$\Delta H_{demic}$ (cal g <sup>-1</sup> )	-0.088	-0.092	
$\Delta H_{demic}$ [cal (mol C <sub>7</sub> F <sub>15</sub> )]	-1100	-2000	

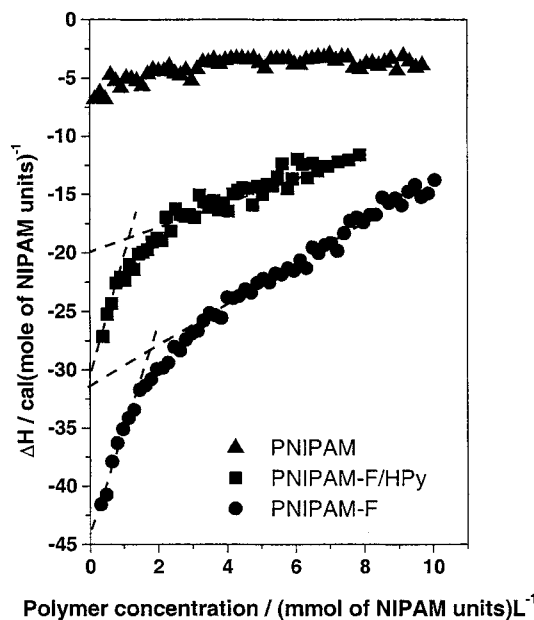
<sup>a</sup> Concentration of onset of aggregation (see Experimental Section). <sup>b</sup> Concentration of end of aggregation (see Experimental Section).

<sup>c</sup> Values cannot be determined experimentally. The heat of dilution of the copolymer is very small as a consequence of the opposite solvation enthalpies of pyrene and octadecyl groups (Raju, B.; Winnik, F. M. Unpublished results). <sup>d</sup> From ref 7.

ppm that is due to the resonance of the terminal methyl protons of the *n*-octadecyl chains. Moreover, the <sup>19</sup>F NMR spectra of PNIPAM-F or PNIPAM-F/HPy solutions in D<sub>2</sub>O were broadened beyond recognition, when measured under conditions similar to those used to measure spectra of the polymers in CDCl<sub>3</sub>. The loss of resolution indicates that the motion of the hydrocarbon and fluorocarbon groups is highly restricted, an occurrence which points to the existence of polymeric micelles.<sup>29</sup> The formation of micellar structures in aqueous solutions of the modified polymers was ascertained by dynamic light scattering measurements. The experiments were carried out at fixed angle (90°) with solutions of the copolymers (1.0 g L<sup>-1</sup>) at 25 °C. Strong signals were obtained, indicating the presence of polymeric micelles, in contrast to the solutions of PNIPAM, which gave no measurable signal. The size of the aggregates, reported in effective diameters (Table 4) ranges from 20 to 38 nm. The diameters of the fluorinated copolymers PNIPAM-F and PNIPAM-F/HPy, are smaller than the value obtained for PNIPAM-HPy. This difference may be attributed to differences in molecular weight among the various samples (Table 1). Alternatively, it may indicate a closer packing of the hydrophobic microdomains in the case of fluorocarbon-modified copolymers.

Further information on the aggregation of HM-PNIPAM samples in water was provided by isothermal titration calorimetry (ITC) experiments carried out at 25 °C. In a typical measurement, aliquots of a concentrated aqueous polymer solution were injected into water at constant temperature. The heat evolved after each injection was measured, and the area under each peak was plotted against the polymer concentration in the calorimeter sample cell. When a concentrated PNIPAM aqueous solution is added to water, the heat evolved was nearly independent of concentration. It corresponds to the heat of dilution,  $\Delta H_{dil}$ , of the polymer. From the enthalpogram recorded during the addition of a 5.0 g L<sup>-1</sup> PNIPAM solution (Figure 6), we obtained  $\Delta H_{dil} \sim -5$  cal mol<sup>-1</sup> NIPAM unit.

Next, we titrated solutions of the hydrophobically modified PNIPAM samples into water. The correspond-

**Figure 6.** Dilution enthalpograms for solutions of PNIPAM, PNIPAM-F and PNIPAM-F/HPy (5 g L<sup>-1</sup>, 25 °C) in water.

ing enthalpograms are presented in Figure 6. They all exhibit marked concentration dependence. In the low concentration regime (<4 mmol NIPAM units L<sup>-1</sup>), the heat evolved is large, but it decreases rapidly with increasing concentration to level off at high concentration. The enthalpogram reflects the following events. After the first few injections, the large enthalpic effect corresponds to the dilution of polymeric aggregates, demicellization of the aggregates, and dissolution of the individual polymer chains. As more polymer solution is added, there comes a point, beyond the critical aggregation concentration, for which the aggregates no longer dissociate and the heat measured is due only to the dilution of the polymeric micelles. The process described is analogous to the demicellization of surfactants, which has been studied extensively by ITC.<sup>30</sup> However unlike surfactants which associate via a highly cooperative mechanism, the hydrophobically modified polymers

Table 5. Fluorescence Lifetimes of the Pyrene-Labeled Polymers in Water (25 °C)

polymer	temp (°C)	$I_E/I_M$	pyrene monomer		pyrene excimer	
			$\tau$ (ns)	$f$	$\tau$ (ns)	$f$
PNIPAM-HPy	25	1.10	28.2	0.29	23.6	-0.28
			121.4	0.71	29.5	0.28
					80.8	0.72
PNIPAM-F/HPy	25	0.62	$\langle\tau\rangle = 94.4$	$(\chi^2 = 1.04)$	$\langle\tau\rangle = 66.4$	$(\chi^2 = 1.04)$
			27.7	0.24	86.7	1
			126.9	0.76		
PNIPAM-F/HPy	29	0.70	$\langle\tau\rangle = 104.4$	$(\chi^2 = 1.09)$		$(\chi^2 = 1.08)$
			24.9	0.26	86.1	1
			115.9	0.74		
	35	0.50	$\langle\tau\rangle = 92.2$	$(\chi^2 = 1.09)$		$(\chi^2 = 1.07)$
			37.0	0.29	82.8	1
			147.6	0.71		
			$\langle\tau\rangle = 115.5$	$(\chi^2 = 1.04)$		$(\chi^2 = 1.08)$

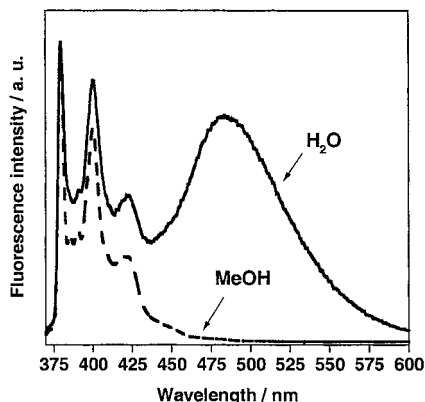


**Figure 7.** Fluorescence spectra of PNIPAM-F/HPy in methanol and in water (polymer concentration, 0.05 g L<sup>-1</sup>; temperature, 25 °C). The spectra are normalized at 376 nm.

assemble via a noncooperative process. Consequently, the enthalpograms recorded for polymer solutions seldom exhibit the sigmoidal shape typical of surfactant dilution but instead show gradual changes of enthalpy with polymer concentration, as observed previously in the cases of hydrophobically modified polyelectrolytes.<sup>31–33</sup> Nonetheless, enthalpograms such as those shown in Figure 6 provide estimates of the enthalpy of demicellization,  $\Delta H_{\text{demic}}$ , and of the polymer concentrations ST and ET of the start and end of transition (see Experimental Section and Figure 2), respectively (Table 4). Comparing data gathered for PNIPAM-F and PNIPAM-F/HPy, we note that, in terms of NIPAM monomer units, the demicellization process is more exothermic in the case PNIPAM-F. However, in terms of fluorocarbon chains, the trend is reversed, given the differences in the levels of fluorocarbon incorporation (Table 1). The concentrations corresponding to the start of the association for solutions of each polymer are low, especially in terms of fluorocarbon concentration ( $[C_7F_{15}] \sim 5\text{--}13 \mu\text{mol}$ ).

#### Photophysical Properties of the Copolymers.

The steady-state fluorescence spectrum of a dilute solution of PNIPAM-F/HPy in water, at 25 °C, consists of two contributions (Figure 7): a well-resolved emission with the (0,0) band located at 376 nm due to locally isolated excited pyrene (pyrene monomer emission, intensity  $I_M$ ) and a strong, broad and featureless emission centered at 478 nm attributed to the emission of pyrene excimer (intensity  $I_E$ ). Measurements carried out as a function of polymer concentration indicated that the strong pyrene excimer emission persists even for solutions of very low concentration ( $<0.01 \text{ g L}^{-1}$ ). Spectra of dilute solutions of PNIPAM-F/HPy in organic solvents

however present only the characteristic pyrene monomer emission, as shown in Figure 7 in the case of methanol. The fact that pyrene excimer emission is so strong for polymer solution in water implies that the pyrene groups are in close spatial proximity. This may be due to a nonstatistical distribution of the pyrene groups along the polymer backbone or to the occurrence of hydrophobic microdomains into which the pyrenes are confined and kept in close proximity. We favor the latter since excimers are barely detectable in spectra recorded from solutions of the same polymer in methanol, where PNIPAM and its hydrophobically modified copolymers are known to exist in an random coil conformation.

While the steady-state emission spectra of PNIPAM-HPy and PNIPAM-F/HPy in water and in methanol present similar features,<sup>1</sup> other spectroscopic properties of the two polymers are quite different. First, the ratio of excimer to monomer emission intensities,  $I_E/I_M$ , is much smaller in the case of PNIPAM-F/HPy (Table 5) even though the level of pyrene incorporation in the two polymers is the same. This observation may hint to an increased dilution of the pyrene chromophores within the hydrophobic domains, rendering the formation of dimers less probable, or else it may tell us that the excimer emission competes with nonemissive deactivation processes, such as pyrene self-quenching. Second, the excitation spectra monitoring the pyrene monomer emission ( $\lambda_{\text{em}} 376 \text{ nm}$ ) or the pyrene excimer emission ( $\lambda_{\text{em}} 478 \text{ nm}$ ) are identical, in the case of PNIPAM-HPy in water,<sup>1</sup> but they are different in the case of PNIPAM-F/HPy. They present the same overall features, but the spectrum recorded for the excimer emission is broader and its maxima are shifted to longer wavelengths by  $\sim 1.0 \text{ nm}$ . These observations are diagnostic of profound differences in the mechanism of pyrene excimer formation and are consistent with an excimer originating from preformed ground-state pyrene aggregates,<sup>34</sup> while in the case of PNIPAM-HPy, all data concur to ascertain that the excimer forms via the more common dynamic process involving an encounter complex between an excited pyrene and a pyrene in its ground state.<sup>35</sup>

To confirm this important difference in the photo-physic of pyrene in solutions of PNIPAM-F/HPy and PNIPAM-HPy, we measured the fluorescence lifetimes of pyrene monomer and excimer emissions from solutions of each polymer in water. As anticipated for static excimer formation, no growing-in component was detected in the profile recorded for the excimer of PNIPAM-F/HPy. Thus, the excimer formation is too fast for detection by the instrument (detection limit 0.2 ns). In the case of PNIPAM-HPy, the excimer profile exhibits a growing-in component ( $\tau 23.6 \text{ ns}$ ) and a decay profile



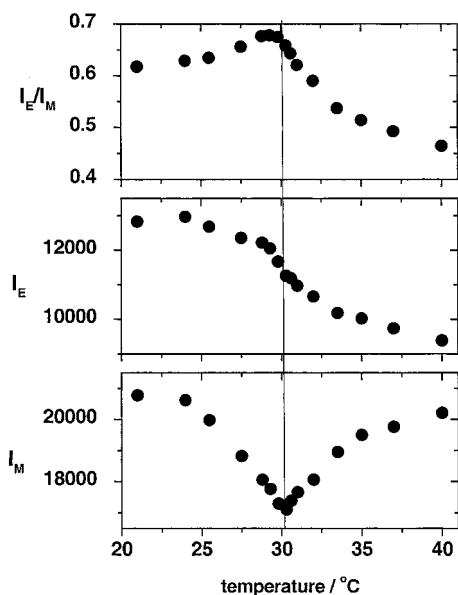


**Figure 8.** Plot of the changes as a function of temperature of the pyrene monomer emission  $I_M$ , the pyrene excimer emission  $I_E$ , and the ratio  $I_E/I_M$  for a solution of PNIPAM-F/HPy in water (polymer concentration:  $0.05 \text{ g L}^{-1}$ ).

that was fitted to a biexponential law, with an average lifetime of 66.4 ns (Table 5). These data are consistent with dynamic excimer formation process. It should be pointed out that most fluorescence measurements were carried out with solutions far less concentrated than those evaluated by ITC, to avoid undesired artifact caused by excessive pyrene concentration. We carried out a study of the changes in  $I_E/I_M$  as a function of polymer concentration from 0.01 to  $1.0 \text{ g L}^{-1}$  for aqueous solutions of and PNIPAM-F/HPy (data not shown). As already observed for solutions of PNIPAM-HPy,<sup>1</sup> the ratio remained constant over the entire concentration range. This result may seem in conflict with the ITC data, which allowed us to identify a polymer concentration, ST, corresponding to the onset of interpolymeric association. While fluorescence experiments characterize the local surrounding of pyrene groups, the ST and ET values reflect macroscopic properties of the solutions. Thus, the two techniques may detect different stages of the development of multichain polymeric micelles.

Next we monitored the changes in pyrene photophysics in a solution of PNIPAM-F/HPy as it is heated through its cloud point. When a solution of PNIPAM-F/HPy was heated from 20 to 40 °C, several spectroscopic events took place (Figure 8). The ratio  $I_E/I_M$  increased slightly to reach a maximum value of 0.68 at 29 °C. It decreased sharply as the solution was heated further and reached a minimum value of 0.45 at 40 °C. The midpoint of the transition is 30 °C, the temperature of macroscopic phase separation. The small increase in  $I_E/I_M$  observed with increasing temperature below the cloud point reflects a decrease in monomer emission intensity in this temperature range (Figure 8). This decrease in monomer emission intensity is consistent with the shortening of the excited pyrene monomer lifetime in this temperature range (Table 5). The decrease in  $I_E/I_M$  upon further increase of temperature reflects a reversal of this trend: the monomer emission intensity and its lifetime increase at the expense of the excimer emission intensity, reflecting the disruption of a fraction of the pyrene aggregates. It is important to note that a significant fraction of the emission of

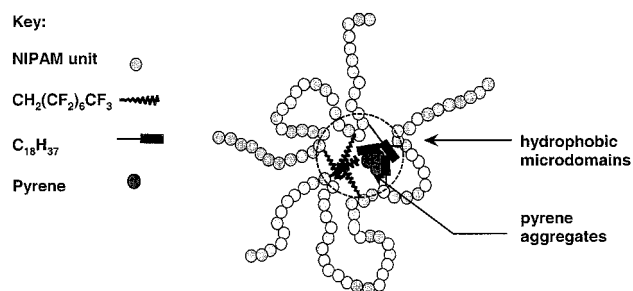


**Figure 9.** Pictorial representation of the morphology of PNIPAM-F/HPy micelles in cold water.

aqueous PNIPAM-F/HPy above its cloud point is due to pyrene excimer emission, and that these excimers originate from preformed pyrene aggregates (see lifetime data, Table 5). Thus, the fluorocarbon/hydrocarbon segregated microdomains persist in the phase separated polymer-rich phase, *unlike* the situation for aqueous solutions of PNIPAM-HPy.<sup>1</sup>

## Conclusion

At the onset of this study, we set about to assess the association in water of a neutral water-soluble polymer bearing both alkylated hydrophobic groups and fluorinated hydrophobic/lipophobic groups and, more specifically, how the presence of fluorinated groups influences the association of the hydrocarbon chains. One can envisage two extreme scenarios: (1) the fluorinated and the alkylated substituents are incompatible and do not mix, as reported in the case of H- and F-poly(acrylamide),<sup>20</sup> or (2) the two types of substituents are miscible and form mixed microdomains. The photophysical experiments were designed to help clarify this point. One should remember that the pyrene group is located in close proximity to a hydrocarbon chain; hence, it will report primarily on the assembly of the H-substituents. If the polymers assemble in water to form distinct fluorocarbon and hydrocarbon microdomains, the photophysical properties of pyrene should not be affected by the presence of fluorocarbon groups. However, if there is some level of intermixing among the F- and H-chains, the properties of pyrene will be greatly affected. The fluorescence data reported in the previous sections are clear: the photophysical properties of pyrene in PNIPAM-HPy and PNIPAM-F/HPy are different; hence, the F-chains affect the association of the H-chains in aqueous PNIPAM-F/HPy even when present only in minute levels. Whether or not the two hydrophobic segments are actually associated within single hydrophobic microdomains cannot be ascertained from the fluorescence data alone.

There have been several reports that pyrene has a poor affinity toward fluorocarbon microdomains.<sup>14,15,20,36,37</sup> Thus, we may anticipate that, within a hydrophobic microdomain, the pyrene groups assemble in close proximity to the hydrocarbon chains and that, to avoid unfavorable interactions with the fluorocarbon chains, they assemble close to each other even though they have to overcome the repulsive interactions among aromatic moieties. An idealized morphology of the hydrophobic F/HPy microdomains is shown pictorially in Figure 9. This description is in agreement with the observation of a "static" pyrene excimer in aqueous solutions of PNIPAM-F/HPy, but not in aqueous PNIPAM-HPy, where the pyrenes are solubilized within the hydrocarbon chains without constraints imposed by the F-chains.



Excimers originating from preformed pyrene ground-state aggregates have been observed previously in aqueous solutions of pyrene-labeled PNIPAM that does not carry other hydrophobic substituents.<sup>38</sup> The differences observed between the thermodynamic characteristics of aqueous PNIPAM-HPy and PNIPAM-F/HPy solutions, especially the enhanced changes in hydration volume for PNIPAM-F/HPy solutions, bring further support to the proposed unique morphology of the hydrophobic micellar core.

**Acknowledgment.** This work was supported in part by a grant of the Natural Sciences and Engineering Council of Canada to F.M.W. and by a fellowship to P.K. from the International Atomic Energy Agency, Vienna, Austria. The authors thank Dr. Bangar Raju (Université de Montréal) for his help in measuring fluorescence lifetimes.

## References and Notes

- (1) Ringsdorf, H.; Venzmer, J.; Winnik, F. M. *Macromolecules* **1991**, *24*, 1678.
- (2) Schild, H. G.; Tirrell, D. A. *Langmuir* **1991**, *7*, 1317.
- (3) Heskins, M.; Guillet, J. E. *J. Macromol. Sci. Chem. A2* **1968**, *1441*.
- (4) Ringsdorf, H.; Simon, J.; Winnik, F. M. *Macromolecules* **1992**, *25*, 5353.
- (5) Ringsdorf, H.; Simon, J.; Winnik, F. M. *Macromolecules* **1992**, *25*, 7306.
- (6) Winnik, F. M.; Winnik, M. A.; Ringsdorf, H.; Venzmer, J.; *J. Phys. Chem.* **1991**, *95*, 2583.
- (7) Winnik, F. M.; Davidson, A. R.; Hamer, G. K.; Kitano, H. *Macromolecules* **1992**, *25*, 1876.
- (8) Winnik, F. M.; Adronov, A.; Kitano, H. *Can. J. Chem.* **1995**, *73*, 2030.
- (9) Yamazaki, A.; Song, J. M.; Winnik, F. M.; Brash, J. L. *Macromolecules* **1998**, *31*, 109.
- (10) Poncet-Legrand, C.; Winnik, F. M. *Polym. J.* **2001**, *33*, 277.
- (11) Spafford, M.; Polozova, A.; Winnik, F. M. *Macromolecules* **1998**, *31*, 7099.
- (12) Principi, T.; Goh, C. C. E.; Liu, R. C. W.; Winnik, F. M. *Macromolecules* **2000**, *33*, 2958.
- (13) Bokias, G.; Hourdet, D.; Iliopoulos, I. *Macromolecules* **2000**, *33*, 2929.
- (14) Li, M.; Jiang, M.; Zhang, Y.-X.; Fang, Q. *Macromolecules* **1997**, *30*, 470.
- (15) Zhang, Y.; Li, M.; Fang, Q.; Zhang, Y.-X.; Jiang, M.; Wu, C. *Macromolecules* **1998**, *31*, 2527.
- (16) Kunieda, H.; Shinoda, K. *J. Phys. Chem.* **1976**, *80*, 2468.
- (17) Zhang, Y.-X.; Huang, F.; Hogen-Esch, T. E.; Butler, G. In *Water Soluble Polymers*; Shalaby, S., McCormick, C., Butler, G., Eds.; American Chemical Society Symposium Series 467; American Chemical Society: Washington, DC, 1991; p 159.
- (18) Lehmann, P.; Ringsdorf, H.; *Int. Symp. Polym. Ther.* **1996**, *78*.
- (19) De Gennes, P. G.; *C. R. Acad. Sci., Ser. II-B* **1999**, *327*, 535.
- (20) Strähler, K.; Selb, J.; Candau, F. *Langmuir* **1999**, *15*, 7565.
- (21) Kujawa, P.; Winnik, F. M. *Macromolecules* **2001**, *34*, 4130.
- (22) *Biocalorimetry, Applications of Calorimetry in the Biological Sciences*; Ladbury, J. E., Chowdhry, B. Z., Eds.; John Wiley & Sons: Chichester, U.K., 1998.
- (23) Fujishige, S. *Polym. J.* **1987**, *19*, 297.
- (24) As the level of perfluorochain incorporation in PNIPAM-F/HPy does not exceed 1 mol %, the contribution of the methylene protons was neglected in the calculations.
- (25) Cochin, D.; Hendlinger, P.; Laschewsky, A. *Colloid Polym. Sci.* **1995**, *273*, 1138.
- (26) Note that this was not the case for copolymers with contents of <sup>1</sup>H,<sup>1</sup>H-perfluorooctyl chains exceeding 1.5 mol %, in agreement with the report of Li et al.,<sup>14</sup> even though a different fluorocarbon chain, 2-(*N*-ethylperfluorooctane sulfonamido) ethyl, was used.
- (27) Israelachvili, J. N. *Intermolecular and Surface Forces*; Academic Press: London, 1985.
- (28) Privalov, P. L.; Griko, Y. V.; Venyaminov, S. Y.; Kutysenko, V. P. *J. Mol. Biol.* **1986**, *190*, 487.
- (29) Xie, X.; Hogen-Esch, T. E. *Macromolecules* **1996**, *29*, 1734.
- (30) See for example: Olofsson, G.; Wang, G. in *Polymer-Surfactant Systems*, Surfactant Science Series 77; Kwak, J. C. T., Ed.; Marcel Dekker: New York, 1998; pp 317–256 and references therein.
- (31) Mizusaki, M.; Morishima, Y.; Raju, B. B.; Winnik, F. M. *Eur. Phys. J. E* **2001**, *5*, 105–115.
- (32) Klijn, J. E.; Kevelam, J.; Engberts, J. B. F. N. *J. Colloid Interface Sci.* **2000**, *226*, 76.
- (33) Bangar Raju, B.; Winnik, F. M.; Morishima, Y. *Langmuir* **2001**, *17*, 4416.
- (34) Winnik, F. M. *Chem. Rev.* **1993**, *93*, 587.
- (35) Birks, J. B. *Rep. Prog. Phys.* **1975**, *38*, 903.
- (36) Kalyanasundaram, K. *Langmuir* **1988**, *41*, 942.
- (37) Almgren, M.; Wang, K.; Asakawa, T. *Langmuir* **1997**, *13*, 4335.
- (38) Winnik, F. M. *Macromolecules* **1990**, *23*, 233.

MA010384T